Grid Impact Evaluation of Localized Geomagnetic Field Enhancements Using Sensitivity Analysis

Yiqiu Zhang, *Student Member, IEEE,* Komal S Shetye, *Senior Member, IEEE,* Adam B. Birchfield*, Student Member, IEEE,* and Thomas J Overbye, *Fellow, IEEE*
Department of Electrical and Computer Engineering
Texas A&M University
College Station, TX, USA
{yzhang458, shetye, abirchfield, overbye}@tamu.edu

***Abstract*—Geomagnetic disturbances (GMDs) can impose great challenges on power system operations due to geomagnetically induced currents (GICs). During the peak periods of a GMD event, geomagnetic fields may substantially increase in some areas. This phenomenon, known as localized geomagnetic field enhancement, causes the localized augmentation of geoelectric fields and the flow of "extra" GICs. Using the principle of superposition, this paper defines a sensitivity associated with the "extra" GICs to quantify the impact of local enhancements on transformers. Sensitivity analysis is performed on a 20-bus benchmark system and a 10k-bus synthetic network, respectively. The results show that "extra" GICs are localized and suggest that the impact scope of a square local enhancement area is generally less than one and a half times its width.**

***Index Terms*--Geomagnetic disturbances (GMDs), geomagnetically induced currents (GICs), localized geomagnetic field enhancement, power system sensitivity analysis, principle of superposition.**

I. INTRODUCTION

Geomagnetic disturbances (GMDs) have the potential to cause great challenges on system operations and damage to grid assets. During solar coronal mass ejection (CME) events, GMDs naturally occur as the injected charged particles interact with the earth's magnetosphere [1], [2]. The disturbed geomagnetic fields produce quasi-dc electric fields with frequencies ranging from 0.01 Hz to 0.5 Hz at ground level [1]. The quasi-dc geoelectric fields then induce dc voltages in transmission lines and cause geomagnetically induced currents (GICs) to flow in the wye-grounded lines [1], [2]. With GICs in the lines, transformers may experience half-cycle saturation, overheating, and even damage [1]-[4]. Voltage collapse may also occur as the result of transformer reactive power absorption and protection device maloperations [1]-[3], [5].

This paper focuses on evaluating the impact of a special GMD phenomenon called localized geomagnetic field enhancement. As suggested in [6], during the peak periods of GMD events, geomagnetic fields may substantially increase in some areas with sides of approximately 100 km in North-South direction and 500 km in East-West direction. With the localized geomagnetic fields increasing, geoelectric fields will also increase in some areas of similar dimensions and induce "extra" GICs. The extent of the impact of these "extra" GICs on power grids has not been fully explored in previous works. Without the local enhancement phenomenon considered, earlier works such as [7] and [8] suggested that GICs are localized. Reference [9] illustrated the regional impact of a local enhancement by statistically showing that only a small set of transformers experience notable changes in GICs in the presence of a local enhancement. Moreover, the case study in [10] exhibited a negative correlation between the distance from a transformer to a local enhancement and the change in GIC experienced by the transformer.

The imposition of GICs on transformers' ac waveforms may cause the transformers to saturate which will change the power flow solution. However, the superposition principle can still be used in GIC calculations, considering that any power grids are seen as dc systems from GICs' point of view. Once the flow of GICs are determined using the superposition principle, their effects on the power flow can be taken into account as additional reactive loads on the saturated transformers. Besides, the application of linear superposition in GIC modeling was justified in [10], [11]. This paper decomposes a local enhancement geoelectric field into a base field and an "extra" field. This paper defines and utilizes a sensitivity associated with the "extra" GICs to quantify the impact of the local enhancement on transformers. The results from sensitivity analyses, performed on a 20-bus benchmark system [12] and a 10k-bus synthetic network, fictitious and not containing any critical electric infrastructure information (CEII), [13]-[15] show that "extra" GICs are localized and suggest that the impact scope of a square local enhancement area is generally less than one and a half times its width.

This paper consists of five sections. Section II summarizes GIC modeling used in [16], [17], [7]. Section III derives the sensitivity used to quantify the impact of local enhancements. Section IV presents the results of the sensitivity analysis conducted on the 20-bus system and 10k-bus system, respectively. Section V concludes the paper.

978-1-7281-0407-2/19/$31.00 ©2019 IEEE

II. Overview of GIC Modeling

This section gives an overview of the GIC modeling used here [16], [17], [7]. According to [18], the GMD induced voltage in line m, symbolized as U_m, can be determined by integrating the geoelectric field along the route of line m

$$U_m = \int_R \vec{E_m} \cdot d\vec{l_m} \tag{1}$$

where $\vec{E_m}$ is the geoelectric field in the line segment $d\vec{l_m}$ and R represents the geographic path of line m. In this paper, a variable with a bar on its top denotes a vector. In the case of a uniform geoelectric field, (1) is equivalent to

$$U_m = E_m L_m \cos(\theta_{E,m} - \theta_{L,m}) \tag{2}$$

where E_m and $\theta_{E,m}$ represents the magnitude (V/km) and direction of the geoelectric field in line m; L_m and $\theta_{L,m}$ represents the length and the direction of line m ("from" bus – "to" bus). In this paper, all the directions are defined in degrees and referred to the north.

Consider a power system containing b buses, s substations, m transmission lines, and r transformers. Let N equal to the sum of b and s. Therefore, the system has N nodes in total which comprise b buses and s substation neutrals. The nodal voltage vector V can be found by using

$$\mathbf{V} = \mathbf{G}^{-1}\,\mathbf{I} \tag{3}$$

where **G** is an N-dimensional symmetric matrix resembling the bus admittance matrix but altered to account for substation neutral buses and substation grounding resistances; **I** is an N-dimensional vector with each entry corresponding to the Norton equivalent dc current injection at a node [17], [7], [19]. With vector **I** broken down, (3) can be modified as

$$\mathbf{V} = \mathbf{G}^{-1}\,\mathbf{B}\,\mathbf{A}\,\mathbf{E} \tag{4}$$

where **E** is an m-dimensional vector with entry m equal to the magnitude of the geoelectric field in line m; **A** is an m-dimensional diagonal matrix with its diagonal entry m equal to the cosine of the angle difference between the geoelectric field and line m; **B** is an N-by-m matrix where column m is associated with line m and only has non-zero values in the rows corresponding to the "from" and "to" buses of line m; each non-zero entry in **B** has a magnitude equal to the product of the three-phase conductance and length of the associated line and follows the sign convention that a positive sign (a negative sign) is assigned to a "from" bus entry ("to" bus entry) [17], [7], [19]. Given the knowledge of all the nodal voltages and line conductances, GIC flowing through any connections can be obtained by using Ohm's law.

The reactive power losses on transformers caused by GICs are modelled as additional reactive loads, which are assumed to vary linearly with the transformers' effective GICs [20], [21]. The effective GIC of a transformer is a function of the transformer's parameters (i.e. turns ratio and structure) and GICs flowing into both of the windings of the transformer [16], [17], [7], [19]. By introducing a row vector $\mathbf{C}_r$, the effective GIC of transformer r can be determined by solving

$$I_{Eff,r} = |\,\mathbf{C}_r\,\mathbf{V}\,| = |\,\mathbf{C}_r\,\mathbf{G}^{-1}\,\mathbf{B}\,\mathbf{A}\,\mathbf{E}\,| \tag{5}$$

where $\mathbf{C}_r$ is an N-dimensional row vector. $\mathbf{C}_r$ is sparse and only has non-zero values at entries associated with transformer r's windings and substation neutral [7], [19]. Considering that the linearity of (4) has been proved in [10] and the matrix multiplication of $\mathbf{C}_r$ and (4) is essentially a linear operation, the linearity is preserved for the product of $\mathbf{C}_r$ and (4). For simple reference in the later text, define

$$I_{AEff,r} = \mathbf{C}_r\,\mathbf{V} = \mathbf{C}_r\,\mathbf{G}^{-1}\,\mathbf{B}\,\mathbf{A}\,\mathbf{E}. \tag{6}$$

$I_{AEff,r}$ is defined as the "actual effective GIC" of transformer r. The principle of superposition can be applied to any linear operations involving $I_{AEff,r}$.

III. Derivition of Local Enhancement Associated Sensitivity

A uniform geoelectric field cannot be assumed in the presence of a local enhancement, since the geoelectric field inside the local enhancement area is higher in magnitude and even has a different direction than that in the surrounding areas. In this case, the GMD-induced dc voltage in each line can be estimated by summing the segment-wise GMD-induced voltages due to different fields, under the assumption that the field in each segment is uniform [7].

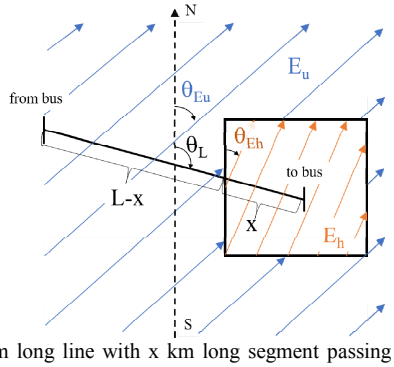

Fig.1. An L km long line with x km long segment passing through a local enhancement area, indicated by the rectangle. The magnitudes and directions of the geoelectric fields inside and outside the area are indicated by the densities and orientations of the orange and blue arrows, respectively.

Refer to Fig.1 and consider a scenario where line m of length L km was originally in a uniform geoelectric field of $E_{u,m}$ V/km and $\theta_{Eu,m}$ degrees. Then, a local enhancement occurs and changes the geoelectric field inside the local enhancement area to $E_{h,m}$ V/km and $\theta_{Eh,m}$ degrees. The segment of line m falling inside the area has a length of x km. Based on [7] and [10], the GMD-induced dc voltage in line m changes to

$$U_{n,m} = \vec{E_{u,m}} \cdot (\vec{L_m} - \vec{x_m}) + \vec{E_{h,m}} \cdot \vec{x_m} \tag{7}$$

where $\vec{E_{u,m}}$ and $\vec{E_{h,m}}$ represents the geoelectric field outside (i.e. the original one) and inside the local enhancement area,

respectively; $\bar{L}_m$ and $\bar{x}_m$ denotes line m and the segment of line m inside the local enhancement area, respectively; $U_{n,m}$ represents the new GMD-induced dc voltage in line m. To facilitate the derivation, define the difference between $\bar{E}_{u,m}$ and $\bar{E}_{h,m}$ as $\bar{E}_{c,m}$, which will be referred as the "extra" field. The extra voltage source in line m, ΔU_m, induced solely by the extra field can be written as

$$\Delta U_m = \bar{E}_{c,m} \cdot \bar{x}_m = E_{c,m}\, x_m \cos(\theta_{Ec,m} - \theta_{L,m}) \tag{8}$$

where $E_{c,m}$ and $\theta_{Ec,m}$ is the magnitude and direction of the extra field in line m. Since [10] has justified that a GIC induced by all electric fields together equals to the combination of GICs induced by each individual electric field, the GIC flowing in line m is the sum of the GICs induced by the extra field and by base field, respectively.

Given (6) and (8), the change in the actual effective GIC of transformer r can be determined by solving

$$\Delta I_{AEff,r} = \mathbf{C}_r \Delta \mathbf{V} = \mathbf{C}_r\, \mathbf{G}^{-1}\, \mathbf{B}\, \mathbf{\Sigma}\, \mathbf{A}_c\, \mathbf{E}_c \tag{9}$$

where $\Delta I_{AEff,r}$ is the extra actual effective GIC of transformer r caused solely by the extra field, which will be referred to as EAE_r; $\mathbf{\Sigma}$ is an m-dimensional diagonal matrix with entry m on the diagonal equal to the ratio of line m passing through the local enhancement area; $\mathbf{A}_c$ is an m-dimensional diagonal matrix with its diagonal entry m equal to the cosine of the angle difference between the extra field and line m; $\mathbf{E}_c$ is an m-dimensional vector with entry m equal to the magnitude of the extra field in line m. For simplicity of notation, define the following row vector for transformer r

$$\frac{d\Delta I_{AEff,r}}{d\mathbf{E}_{c,T}} = \mathbf{C}_r\, \mathbf{G}^{-1}\, \mathbf{B}\, \mathbf{\Sigma} = \mathbf{S}_{c,T,r} \tag{10}$$

where $\mathbf{E}_{c,T}$ is an m-dimensional vector with entry m equal to the magnitude of the extra field tangent to line m; $\mathbf{S}_{c,T,r}$ is an m-dimensional row vector with entry m equal to EAE_r with 1 V/km variation in the extra field tangent to line m. Therefore, (9) can be transformed into a summation form

$$\begin{aligned} \Delta I_{AEff,r} &= \mathbf{S}_{c,T,r}\, \mathbf{A}_c\, \mathbf{E}_c \\ &= \sum_{m=1}^{m} (\mathbf{S}_{c,T,r}\,[m] \cos(\theta_{Ec,m} - \theta_{L,m})\, E_{c,m}) \end{aligned} \tag{11}$$

where $\mathbf{S}_{c,T,r}\,[m]$ represents entry m in $\mathbf{S}_{c,T,r}$. Under the assumption that the extra field is uniform in magnitude within the local enhancement area, the sensitivity used to quantify the impact of the local enhancement on transformer r can be defined as

$$\frac{d\Delta I_{AEff,r}}{dE_c} = \sum_{m=1}^{m} (\mathbf{S}_{c,T,r}\,[m] \cos(\theta_{Ec,m} - \theta_{L,m})) \tag{12}$$

where E_c represents the magnitude (assumed uniform) of the extra field. The sensitivity defined in (12) will be referred to as SEAE (sensitivity of the extra actual effective GIC of a transformer). When the extra field is 1 V/km, SEAE of a transformer equals the sum of the EAEs contributed by each individual line. To account for an extra field with a nonuniform magnitude, scaling factors can be combined with corresponding summation terms in (11). In the worst-case local enhancement scenario, the extra field is aligned with every line segment passing through the local enhancement area and oriented properly to maximize the SEAE. Regardless of the likelihood of the worst-case scenario, the worst-case SEAE can be used as the upper limit of SEAE when the consideration of angle differences is not preferred. During local enhancement GMD event, the effective GIC of transformer r can be determined by using superposition

$$I_{Eff,r,n} = |\, I_{AEff,r,u} + \Delta I_{AEff,r}\,| \tag{13}$$

where $I_{Eff,r,n}$ represents the effective GIC of transformer r; $I_{AEff,r,u}$ is the part of the actual effective GIC contributed by the uniform base field; $\Delta I_{AEff,r}$, or EAE_r, is the part of the actual effective GIC contributed by the extra field. Equation (13) can be further generalized to account for multiple local enhancements by adding more $\Delta I_{AEff,r}$ terms associated with different local enhancements. Moreover, SEAEs can be determined to facilitate the calculation of the effective GICs. Thus, equation (13) provides a flexible and prompt way of analyzing the impact of local enhancements by decoupling the impact of the base field and that of the extra field.

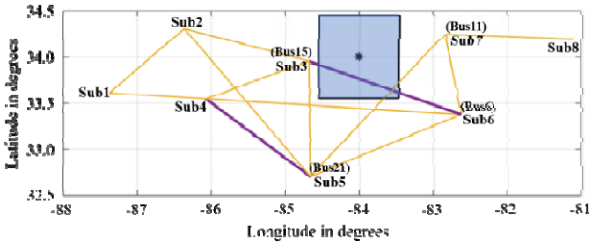

Fig.2. A geographic view of a 20-bus system with the shaded area indicating the local enhancement area. The locations of all substations and some buses of interest (in parentheses) are shown.

IV. Case Studies

A. 20-bus Benchmark System

A 20-bus benchmark system developed in [12] is used for the local enhancement impact study in this section. A geographic view of the 20-bus system is shown in Fig.2. The yellow lines and purple lines represent the single-circuit lines and double-circuit lines, respectively. A local enhancement occurs in a 100 km by 100 km area, indicated by the shaded rectangle centered at (34° N, 84° W). Assume that a uniform base geoelectric field of 1 V/km is applied to the footprint shown in Fig.2, except the local enhancement area. The geoelectric field inside the local enhancement area has a magnitude of 2 V/km and the same direction of the base field. The base field and local enhancement field are rotated simultaneously from 0 to 360 degrees in increments of 10

degrees so that the extra field is always 1 V/km in the same direction of the base field.

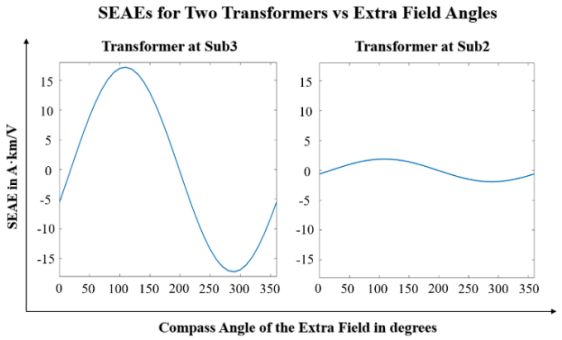

Fig.3. The variation in SEAE for the transformer at substation 3 and transformer at substation 2 as the 1 V/km extra field varies from 0 to 360 degrees in steps of 10 degrees.

The autotransformer at substations 3 and generator step-up (GSU) transformer at substation 2 is located 51 km and 220 km away from the center of the local enhancement area, respectively. For the transformer at substations 3 and transformer at substation 2, SEAE is shown in the left plot and right plot in Fig.3, respectively, as a function of the compass angle of the extra field. The significant magnitude difference shown in Fig.3 implies that the impact of the local enhancement on the transformers decreases rapidly as the distances between them increase. It is worth noting that even though the plots in Fig.3 appear to be in phase, this observation is not universal and only occurs due to the limited size of the system.

TABLE I
SEAE AND CONTRIBUTION FROM LINES TO EAE FOR TWO TRANSFORMERS UNDER EASTWARD EXTRA FIELD

	Transformer at Sub 3	Transformer at Sub 2
SEAE	16.32	1.80
EAE From Line 15-6,1	8.16	0.90
EAE From Line 15-6,2	8.16	0.90
EAE From Line 21-11	0	0

Next, with the extra field fixed at 90 degrees (eastward), EAEs contributed by lines are recorded in Table I for the transformer at substation 3 and transformer at substation 2 in the second column and third column, respectively. As the lines making zero EAE contribution are omitted from Table I, it is found that only three lines, which pass through the local enhancement area, make contributions to EAEs. Line 21-11 is not omitted from Table II, because the values of EAEs contributed by line 21-11 (on the order of 10-6) are rounded to zero. Since the magnitude of the extra field is 1 V/km, the EAE contributed by each of the lines corresponds to a summation term in (11). Therefore, as shown in the second row of Table I, the SEAE for each of the transformers can be obtained by summing the EAEs contributed by the three lines listed in the corresponding column.

In reference to Fig.2, line 15-6,1 and line 15-6, 2 comprise the double-circuit line (in purple) between substation 3 and substation 6, while the line 21-11 comprises the single-circuit line (in yellow) between substation 5 and substation 7. It is observed that the EAEs contributed by line 15-6,1 and line15-6,2 are much higher than that contributed by line 21-11 (small enough to be grounded to zero) for both of the transformers. Line 15-6,1 and line 15-6,2 are found to have much longer segments passing through the local enhancement area than line 21-11. This observation suggests that lines with longer segments passing through a local enhancement area tend to contribute greater EAEs than lines with shorter segments. In other words, a local enhancement tends to impact transformers through lines with longer segments passing through the local enhancement area. It is worth noting that the foregoing is just a tendency, since the values of EAEs also depend on the angle differences between the lines and extra field, based on (11).

B. 10k-bus Synthetic Network

In this section, sensitivity analysis is conducted on a 10k-bus synthetic network [13]-[15] in two stages. In stage one, five local enhancement areas with different locations and dimensions are applied to the system individually. The impact scope of each local enhancement is evaluated using the worst-case SEAE. In stage two, SEAEs for six selected transformers are determined, as the extra geoelectric field varies in direction.

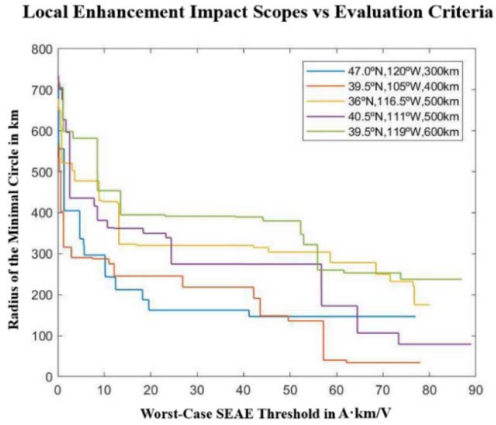

Fig.4. The impact scopes of the five selected local enhancements versus different evaluation criteria (thresholds) with which the worst-case SEAEs of transformers are compared to determine whether the transformers are under impact.

The motivation for stage one is to investigate the relationship between the physical characteristics such as location and dimension of a local enhancement and its impact scope. The worst-case SEAE is preferred over SEAE to isolate the dependence on the angle differences between the lines and extra field. Therefore, it is unnecessary to specify the magnitude and direction of the extra field here. 0.1 A·km/V and 1 A·km/V are arbitrarily chosen as the thresholds with which the worst-case SEAE of each transformer is compared to determine whether the transformer is classified as impacted by the local enhancement. The impact scope of a local enhancement is quantified by the radius of the smallest circle or minimal circle that contains all the transformers with their worst-case SEAEs exceeding the threshold. Five square local enhancement areas, with their centers and widths shown in the

first and second rows of Table II, are selected and applied to the system individually.

TABLE II
IMPACT SCOPES OF FIVE LOCAL ENHANCEMENTS BASED ON DIFFERENT EVALUATION CRITERIA

Local Enhancement Center	47º N, 120º W	39.5º N, 105º W	36º N, 116.5º W	40.5º N, 111º W	39.5º N, 119º W
Local Enhancement Width (km)	300	400	500	500	600
Radius of the Minimal Circle (km) (Threshold = 0.1 A·km/V)	726	565	678	735	718
Ratio of the Radius to the Width (Threshold = 0.1 A·km/V)	2.42	1.41	1.36	1.47	1.20
Radius of the Minimal Circle (km) (Threshold = 1 A·km/V)	556	403	521	675	706
Ratio of the Radius to the Width (Threshold = 1 A·km/V)	1.85	1.00	1.04	1.35	1.18

The impact scopes for the five local enhancements are shown in the third and fifth rows, respectively, based on the two impact evaluation criteria (0.1 and 1 A·km/V). To illustrate the relationship between the impact scope and the dimension of the local enhancements, the ratio of the radius of the minimal circle to the width of the local enhancement is determined and presented in the fourth and sixth rows of Table II. It is observed in Table II that the impact scopes of most of the local enhancements are similar in size to the local enhancements themselves. To be specific, the radii of their impact scopes are less than 1.5 times their own widths, even given a conservative evaluation criterion. However, an exception is also observed in this study that the smallest local enhancement (300 km by 300 km) has a comparatively large impact scope with respect to its size (1.85 times its width based on the 1 A·km/V criterion and 2.42 times its width based on the 0.1 A·km/V criterion).

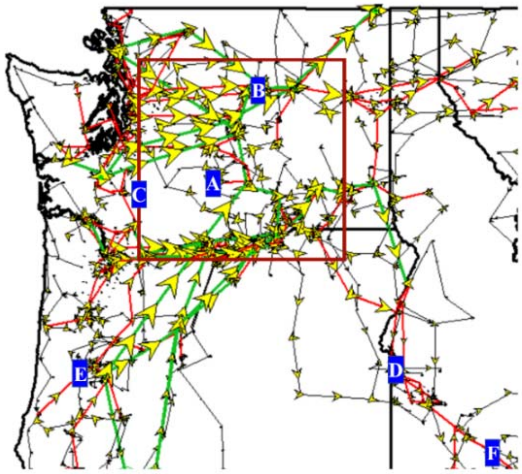

Fig.5. A portion of the 10k-bus synthetic system. The boundary of the 300 km by 300 km local enhancement area is indicated by the red square. The electric fields inside and outside the area are 2 V/km and 1 V/km, respectively, and both of 90 degrees. The yellow arrows represent GICs and A-F fields show the locations of the selected transformers.

It is found that multiple high-voltage (765 kV) long-distance transmission lines emanating from the local enhancement area bring its impact farther through the power grid. To avoid electric field concentration, long-distance high-voltage transmission lines are designed with lower resistances and subject to higher GICs [1], [22]. Therefore, the worst-case SEAEs for the transformers with close electrical connections to these lines are high. Considering that the impact scope of a local enhancement will change given various thresholds, Fig.4 provides an approximate mapping between the impact scopes and evaluation criteria for the five local enhancements for different practical considerations.

In stage two, six transformers are selected to undertake the same sensitivity analysis performed on the 20-bus system from the previous section. The same GMD scenario is taken here, but with the center and width of the square local enhancement area changed to (47º N, 120º W) and 300 km. Fig.5 shows the portion of the 10k-bus system that includes the power grids in Washington, Oregon, Idaho, and Montana. The boundary of the local enhancement area is marked by the red square and the locations of the six selected transformers are indicated as the A-F text fields. The yellow arrows in Fig.5 show the magnitudes and directions of the GICs, where the system is subjected to a 90-degree base field and extra field. It is observed that the high-voltage transmission lines (765kV lines are in green and 345kV lines are in red in Fig.5.) are subjected to high GICs.

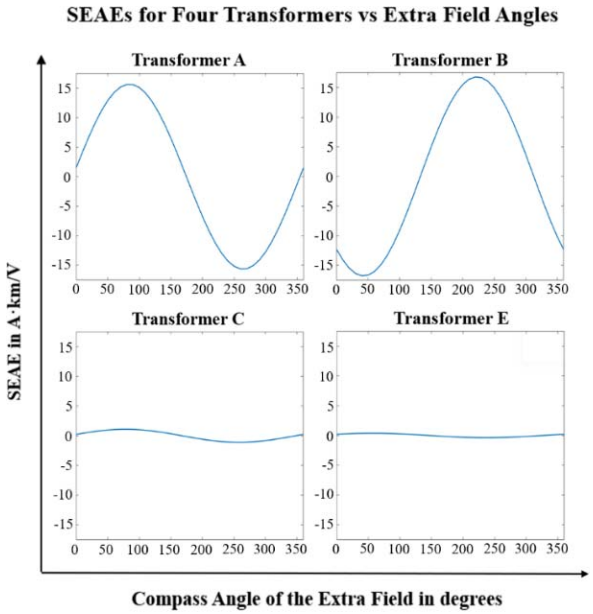

Fig.6. The variation in SEAE for the transformer A, B, C, and E with the compass angle of the extra field ranging from 0 to 360 degrees.

SEAE is determined for each of the six selected transformers as the extra field varies in direction from 0 to 360 degrees in increments of 10 degrees. The SEAEs for transformers D and F are found to be negligible and not explicitly presented here, while the SEAEs for the rest of the transformers are presented in Fig.6. It is observed in Fig.6 that the transformers inside the local enhancement area have much higher magnitudes than those for the ones outside the area. This indicates that the impact of a local enhancement area doesn't propagate far outside the area. In this specific case, transformer F, located about 600km away from the center of the local enhancement area, is not impacted anymore. This result is consistent with the observation made in stage one where worst-case SEAEs were used to measure the impact. However, it is worth noting that the plot for transformer C, outside but near the boundary, has a similar magnitude as that for transformers E, far from the boundary. This observation indicates that a transformer's proximity to a local enhancement does not guarantee a large impact of the local enhancement on the transformer, since various factors such as the voltage level of the transformer, orientations of the lines, and physical characteristics of the local enhancement area all affect the degree of impact. Yet, at first glance, the distance between a transformer and a local enhancement area gives a reasonable approximation for the likelihood of the transformer being impacted.

V. CONCLUSION

This paper investigated the impact of localized geomagnetic field enhancements on transformers using the superposition principle. SEAEs are defined for transformers to quantify the impact of local enhancements on them and to facilitate the computation of their effective GICs. The results of the sensitivity analysis, conducted respectively on a 20-bus system and a large-scale 10k-bus system, suggest that the impact scope of a square local enhancement is generally less than 1.5 times its width. An exception may occur when high-voltage long-distance transmission lines emanate from the local enhancement area and propagate the impact farther out (The studied example showed that the impact scope of such a square local enhancement area might reach 2.5 times its width.).

ACKNOWLEDGMENT

This work was supported by the National Science Foundation (NSF) under Award Number NSF 15-20864.

REFERENCES

[1] V. D. Albertson, J. M. Thorson, R. E. Clayton and S. C. Tripathy, "Solar-Induced-Currents in Power Systems: Cause and Effects," in *IEEE Transactions on Power Apparatus and Systems*, vol. PAS-92, no. 2, pp. 471-477, March 1973.

[2] W. A. Radasky, "Overview of the impact of intense geomagnetic storms on the U.S. high voltage power grid," *2011 IEEE International Symposium on Electromagnetic Compatibility*, Long Beach, CA, USA, 2011, pp. 300-305.

[3] V. D. Albertson, J. M. Thorson and S. A. Miske, "The Effects of Geomagnetic Storms on Electrical Power Systems," in *IEEE Transactions on Power Apparatus and Systems*, vol. PAS-93, no. 4, pp. 1031-1044, July 1974.

[4] D. H. Boteler and E. Bradley, "On the Interaction of Power Transformers and Geomagnetically Induced Currents," in *IEEE Transactions on Power Delivery*, vol. 31, no. 5, pp. 2188-2195, Oct. 2016.

[5] J. G. Kappernman and V. D. Albertson, "Bracing for the geomagnetic storms," in *IEEE Spectrum*, vol. 27, no. 3, pp. 27-33, March 1990.

[6] "Supplemental Geomagnetic Disturbance Event Description, " Project 2013-03 GMD Mitigation, NERC, June. 2017. [Online]. Available: http://www.nerc.com/pa/Stand/Project201303GeomagneticDisturbanceMitigation/Supplemental_GMD_Event_Description_June_2017.pdf.

[7] T. J. Overbye, K. S. Shetye, T. R. Hutchins, Q. Qiu and J. D. Weber, "Power Grid Sensitivity Analysis of Geomagnetically Induced Currents," in *IEEE Transactions on Power Systems*, vol. 28, no. 4, pp. 4821-4828, Nov. 2013.

[8] R. J. Pirjola, "On the flow of geomagnetically induced currents in an electric power transmission network," Canadian J. Phys., vol. 88, no. 5, pp. 357–363, May 2010.

[9] "Benchmark Geomagnetic Disturbance Event Description, " Project 2013-03 GMD Mitigation, NERC, Dec. 2014. [Online]. Available: http://www.nerc.com/pa/Stand/Project201303GeomagneticDisturbanceMitigation/Benchmark-GMD-Event-Dec5-redline.pdf

[10] D. H. Boteler, "The use of linear superposition in modelling geomagnetically induced currents," *2013 IEEE Power & Energy Society General Meeting*, Vancouver, BC, 2013, pp. 1-5.

[11] D. H. Boteler, Q. Bui-Van and J. Lemay, "Directional sensitivity to geomagnetically induced currents of the Hydro-Quebec 735 kV power system," in *IEEE Transactions on Power Delivery*, vol. 9, no. 4, pp. 1963-1971, Oct 1994.

[12] R. Horton, D. Boteler, T. J. Overbye, R. Pirjola and R. C. Dugan, "A Test Case for the Calculation of Geomagnetically Induced Currents," in *IEEE Transactions on Power Delivery*, vol. 27, no. 4, pp. 2368-2373, Oct. 2012.

[13] A. B. Birchfield, T. Xu, K. M. Gegner, K. S. Shetye and T. J. Overbye, "Grid Structural Characteristics as Validation Criteria for Synthetic Networks," in *IEEE Transactions on Power Systems*, vol. 32, no. 4, pp. 3258-3265, July 2017.

[14] T. Xu, A. B. Birchfield, K. S. Shetye and T. J. Overbye, "Creation of synthetic electric grid models for transient stability studies," *2017 IREP Symposium Bulk Power System Dynamics and Control*, Espinho, Portugal, 2017, pp. 1-6.

[15] Electric Grid Test Case Repository (2017). [Online]. Available: https://electricgrids.engr.tamu.edu/electric-grid-test-cases/activsg10k/.

[16] V. D. Albertson, J. G. Kappenman, N. Mohan and G. A. Skarbakka, "Load-Flow Studies in the Presence of Geomagnetically-Induced Currents," in *IEEE Transactions on Power Apparatus and Systems*, vol. PAS-100, no. 2, pp. 594-607, Feb. 1981.

[17] T. J. Overbye, T. R. Hutchins, K. Shetye, J. Weber and S. Dahman, "Integration of geomagnetic disturbance modeling into the power flow: A methodology for large-scale system studies," *2012 North American Power Symposium (NAPS)*, Champaign, IL, 2012, pp. 1-7.

[18] D. H. Boteler and R. J. Pirjola, "Modelling geomagnetically induced currents produced by realistic and uniform electric fields," in *IEEE Transactions on Power Delivery*, vol. 13, no. 4, pp. 1303-1308, Oct 1998.

[19] Hao Zhu and T. Overbye, "Blocking device placement for mitigating the effects of geomagnetically induced currents," *2016 IEEE Power and Energy Society General Meeting (PESGM)*, Boston, MA, 2016, pp. 1-1.

[20] R. A. Walling and A. N. Khan, "Characteristics of transformer exciting-current during geomagnetic disturbances," in *IEEE Transactions on Power Delivery*, vol. 6, no. 4, pp. 1707-1714, Oct 1991.

[21] Xuzhu Dong, Yilu Liu and J. G. Kappenman, "Comparative analysis of exciting current harmonics and reactive power consumption from GIC saturated transformers," *2001 IEEE Power Engineering Society Winter Meeting. Conference Proceedings (Cat. No.01CH37194)*, Columbus, OH, 2001, pp. 318-322 vol.1.

[22] W. A. Radasky and J. G. Kappenman, "Impacts of geomagnetic storms on EHV and UHV power grids," *2010 Asia-Pacific International Symposium on Electromagnetic Compatibility*, Beijing, 2010, pp. 695-698.